Chemical Engineering Journal 106 (2005) 1–12

Chemical Engineering Journal

www.elsevier.com/locate/cej

Activated carbons from lignin: kinetic modeling of the pyrolysis of Kraft lignin activated with phosphoric acid

Daniel Montané*, Vanessa Torné-Fernández, Vanessa Fierro

Department of Chemical Engineering-ETSEQ, Rovira i Virgili University, Av. Països Catalans 26, E-43007 Tarragona, Catalunya, Spain

Received 26 April 2004; received in revised form 19 October 2004; accepted 4 November 2004

Abstract

A phenomenological kinetic model has been developed for the pyrolysis at low heating rates of lignin activated with phosphoric acid. The model is based on thermogravimetry (TG) and differential thermogravimetry (DTG) data from pyrolysis experiments and assumes that lignin carbonization proceeds through a set of pseudo-first-order reactions. These reactions are a simplified description of the multiple reactions involved in the process. TG experiments were performed in nitrogen atmosphere for lignin (L) impregnated with 85% phosphoric acid (PA) at mass ratios (PA:L) from 1.0:1.0 to 1.75:1.0, a typical heating rate of 10 °C/min and a maximum carbonization temperature of 650 °C, including isothermal stages at 150 and 300 °C in the temperature programs for some of the experiments. Analysis of the TG and DTG curves led to a kinetic model that includes an initial reaction step between lignin and phosphoric acid, water formation from the dehydration of the excess of phosphoric acid to P_2O_5, pyrolysis of lignin to carbon and volatiles, evaporation of water and P_2O_5 and finally, partial volatilization of the carbon to light gases. Activation energies and the other parameters of the model were adjusted from experimental data. Activation energies were 26.0 kJ/mol for water desorption, 72.0 kJ/mol for the dehydration of phosphoric acid to phosphoric pentoxide, 95.0 kJ/mol for the volatilization of P_2O_5, 47.7 kJ/mol for the carbonization of the activated lignin and 106.3 kJ/mol for the pyrolytic release of light gases from activated carbon. The model provides a good representation of the thermograms regardless of the phosphoric acid to lignin ratio and the temperature profile along the reaction.

Keywords: Lignin; Activated carbon; Phosphoric acid; Pyrolysis; Kinetics; Thermogravimetric analysis

1. Introduction

Activated carbons are adsorbents that are used industrially in multiple processes for product separation and purification, and for the treatment of liquid and gaseous effluents. Their versatility allows a wide range of uses if their pore size distribution and surface properties are properly tailored, and new applications are being developed in areas such as pollution prevention, supported catalysts and the storage of gaseous fuels such as natural gas and hydrogen. Activated carbons are produced from a wide variety of carbonaceous materials, including wood and agriculture by-products [1], but the expanding market for activated carbons has prompted interest in finding complementary sources of carbonaceous precursors for their manufacture. Using carbonaceous residues and by-products from existing industrial processes as feedstock for producing activated carbons is an attractive strategy that may help reduce costs through process integration. Among several possibilities, lignin, produced as a residual material in the manufacture of cellulose pulps, offers strong potential because it is available in high amounts at low cost. Lignin is the most abundant natural polymer after cellulose. Typically, it represents around 20–30% of the mass of dry wood and is nowadays produced in huge amounts as a by-product in the production of high-quality cellulose pulps, mainly in the Kraft pulping process. In this process, lignin is used as fuel to provide steam for the plant, which also allows the recovery of the pulping chemicals (NaOH and Na_2S). The trend towards larger plant capacities and the op-

* Corresponding author. Tel.: +34 977 559 652; fax: +34 977 558 544.
E-mail address: dmontane@etseq.urv.es (D. Montané).

1385-8947/$ – see front matter © 2004 Elsevier B.V. All rights reserved.
doi:10.1016/j.cej.2004.11.001

Table 1
Lignin analysis (wt.%)

Proximate analysis (wt.%, wet basis)		Ultimate analysis (wt.%, ash and moisture free)	
Moisture	14.45	Carbon	59.46
Ash	9.50	Hydrogen	5.07
Volatile matter	44.93	Nitrogen	0.05
Fixed carbon[a]	31.12	Sulfur	2.15
		Oxygen[a]	33.27

[a] Estimated by difference.

timization of the pulping process to improve cost effectiveness have led to the plants producing more by-product lignin than the amount that is needed to cover their energy consumption. Using Kraft lignin as raw material for chemicals has therefore attracted considerable attention. Several applications for the lignin obtained from pulping processes have been considered. One of its main uses so far has been as a phenol substitute in the formulation of phenol–formaldehyde resins and adhesives, but one of the main areas for possible applications for by-product lignin is in the preparation of activated carbons. The physical activation with CO_2 of pyrolyzed lignins [2,3], as well as chemical activation of lignin with $ZnCl_2$ [4], have been studied, but the use of $ZnCl_2$ is declining due to its environmental impact [5], and phosphoric acid is the preferred activating agent. However, the activation of lignin with phosphoric acid has not been widely investigated, though maximum surface areas of above 1300 m^2/g have been reported [6]. We recently studied the characteristics of the carbons obtained from Kraft lignin activated with phosphoric acid at several process conditions and showed that carbons with high surface areas and good properties can be obtained [7]. In this paper, we study the rates of carbonization of Kraft lignin activated with phosphoric acid in a thermobalance and propose and test a phenomenological kinetic model with the experimental data.

2. Experimental

A sample of Kraft lignin was obtained from Lignotech Ibérica S.A. (Spain) and used to prepare activated carbons as received (see Table 1 for composition). Elemental analysis was performed in a EA1108 Carlo Erba analyzer and the proximate analysis was developed according to ISO standards for moisture (100 °C in air), volatile matter (900 °C in nitrogen atmosphere) and ash (incineration at 815 °C in air).

Phosphoric acid (85% solution, Panreac, Spain) was used as activating agent. Lignin and phosphoric acid were mixed at the desired ratio and the mixture was left for 1 h to allow a complete impregnation of the lignin [8]. A small sample (around 30–50 mg) of the mixture was then transferred to the thermobalance (Perkin-Elmer TGA-7), where pyrolysis was carried out in nitrogen at a constant flow rate of 50 mL/s. Table 2 lists all the other specific conditions for the experiments, which were performed randomly except for a first series, which was performed to establish the reproducibility of the TG results.

3. Results and discussion

Our first set of experiments tested the reproducibility of our experimental procedure. Fig. 1 shows the thermograms (f versus t) and the differential thermograms (df/dt versus t) for replicated experiments on the carbonization of a sample of lignin impregnated with a phosphoric acid to lignin mass ratio (PA/L) of 1.4, a heating rate of 10°/min and a final temperature of 650 °C for 120 min (experiments #10/3, #10/4 and #10/5 in Table 2). Since our experiments included isothermal periods, either at the end of the heating ramp or intercalated in it, we preferred time instead of temperature as the independent variable for our calculations. The average value for the final mass fraction was 0.384 ± 0.014 (95% probability level), which shows the good reproducibility of the ex-

Table 2
Experimental conditions used for the TGA experiments

Run ID	H_3PO_4 (85%) to lignin mass ratio	Initial temperature (°C)	Heating rate (°C/min)	First stage		Second stage		Third stage	
				T (°C)	Time (min)	T (°C)	Time (min)	T (°C)	Time (min)
Exp #10/3	1.4	25	10	650	120	–	–	–	–
Exp #10/4	1.4	25	10	650	120	–	–	–	–
Exp #10/5	1.4	25	10	650	120	–	–	–	–
Exp #2	1.4	25	10	150	15	650	0	–	–
Exp #3	1.4	25	10	150	30	650	30	–	–
Exp #5	1.4	25	10	150	60	650	120	–	–
Exp #13	1.4	25	10	150	60	650	120	–	–
Exp #18	1.4	25	10	300	60	650	120	–	–
Exp #20	1.4	25	10	150	60	300	60	650	120
Exp #21	1.4	25	10	300	60	500	60	750	60
Exp #24	1.4	150	150	650	120	–	–	–	–
Exp #10 (L/P 1:1.0)	1.0	25	10	650	30	–	–	–	–
Exp #14 (L/P 1:1.4)	1.4	25	10	600	120	–	–	–	–
Exp #18 (L/P 1:1.75)	1.75	25	10	650	120	–	–	–	–

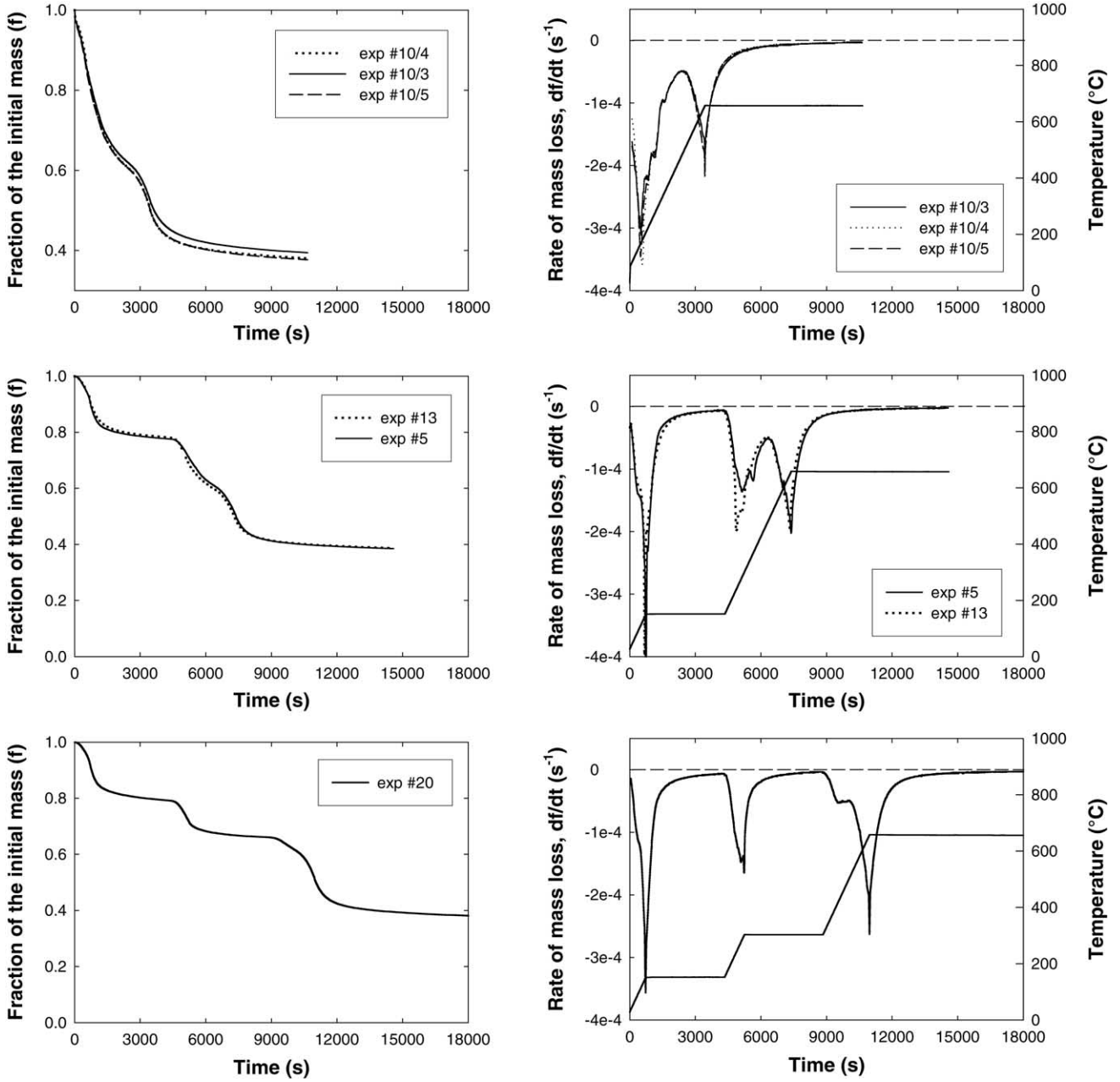

Fig. 1. Effect of the addition of intermediate isothermal stages on the final solid yield and the TG and DTG curves for experiments #5, #10/4 and #20 (experimental conditions listed in Table 2).

periments. The differential thermograms also show excellent agreement among the three experiments throughout the reaction time, since the values of the maximum rates of mass loss and the time at which they are observed are almost identical for the three runs. The differential thermogram shows two peaks for the rate of mass loss. The first starts at low temperature, reaches the maximum rate at around 175–180 °C and extends to 450 °C. The second peak starts at around 500 °C and reaches the maximum rate of mass loss when the isothermal segment at 650 °C starts.

Yoon et al. [9] reported an increase in carbon yield when the sample was maintained at constant temperature for a certain time once the volatilization of the sample had started. Other studies, however, reported that the carbon yield did not change when intermediate isothermal periods were included during the pyrolysis of viscose rayon cloth [10] and apple pulp [11]. We performed experiments #5 and #13, under the same conditions as #10/3, #10/4 and #10/5 but with an isothermal segment at 150 °C for 60 min. Again, reproducibility was excellent for the TG and DTG curves (Fig. 1). The mass fraction remaining at the end of the experiments was 0.386 ± 0.002, which is equivalent to that of the experiments without intermediate isothermal period. We may therefore conclude that including isothermal periods does not signif-

icantly changes the final yield of solid. However, including intermediate isothermal stages proved valuable because it revealed that the peaks of the rate of mass loss in the DTG were the result of the superposition of several reactions. For example, if we compare the DTG plots for experiments #10/4 and #5 we can see that the broad peak observed during the heating period in experiment #10/4 splits into two different peaks when an intermediate isothermal period at 150 °C is added. The new peak shows the maximum rate of mass loss at 350–400 °C, but it appears also to be the result of the superposition of two reactions. This is confirmed by experiment #20, which adds two isothermal periods — one at 150 °C for 60 min and another at 300 °C for 60 min — and shows the existence of four maximums in the rate of mass loss along the thermogram. This experiment also had a yield of residual solid of 0.381, which confirmed that including intermediate isothermal stages has no significant effect on the final mass fraction if the same final temperature of carbonization is achieved.

4. Modeling of lignin pyrolysis

Several models are available in the bibliography for the kinetics of the thermal decomposition of biomass and its fractions. The most usual approach starts with the assumption that the components of biomass (cellulose, hemicellulose and lignin) react simultaneously and independently of the others through a set of parallel reactions [12–15]. When applied to lignin activated with phosphoric acid, the model is reduced to two parallel and independent reaction processes: the volatilization of the water present in the sample and the carbonization of the phosphoric acid-activated lignin (PL) into activated carbon and volatiles. Water comes from the phosphoric acid solution and the moisture of lignin. This system is described mathematically by Eqs. (1)–(5), where $m_{0_{LP}}$ and m_{0_W} are the initial masses of PL mixture and water, m_{LP} and m_W the actual masses of PL and water at a point along the experiment, m_∞ the residual mass of solid at the end of the thermogram, f the fraction of the initial mass remaining as solid, f_{LP} and f_W the fractions of the initial mass of phosphoric-activated lignin and water, f_{LP_0} and f_{W_0} the same at the beginning of the experiment, α_{LP} and α_W the degrees of transformation for activated lignin and water, and k_{LP} and k_W Arrheiuns rate constants for the volatilization of activated lignin and water.

Water volatilization was assumed to be first-order. Some thermogravimetry studies on lignin pyrolysis propose a first-order reaction process [15–17], but most studies conclude that reaction orders are higher [13,14,18,19]. We therefore assumed that the devolatilization of activated lignin may not be first-order and included the reaction order for activated lignin (a_{LP}) as one of the parameters to be optimized from experimental data, together with the activation energies and the frequency factors. A convenient least-squares objective function to calculate the optimal values of these parameters when using several thermograms, which may combine isothermal and non-isothermal stages, is presented in Eq. (6) for p thermograms with $n(i)$ data points each. f_{ij}^{exp} are the measured values of f, and f_{ij}^{cal} are those calculated with Eqs. (3)–(5) and numerical integration of Eqs. (1) and (2):

$$\frac{d\alpha_{LP}}{dt} = k_{LP}(1-\alpha_{LP})^{a_{LP}} \quad \text{with} \quad \alpha_{LP} = \frac{m_{0_{LP}} - m_{LP}}{m_{0_{LP}} - m_\infty} \tag{1}$$

$$\frac{d\alpha_W}{dt} = k_W(1-\alpha_W) \quad \text{with} \quad \alpha_W = \frac{m_{0_W} - m_W}{m_{0_W}} \tag{2}$$

$$f_{LP} = f_{LP_0} - \alpha_{LP}(f_{LP_0} - f_\infty) \tag{3}$$

$$f_W = f_{W_0}(1-\alpha_W) \tag{4}$$

$$f = f_{LP} + f_W \tag{5}$$

$$F = \sum_{i=1}^{p} \left(\frac{\sum_{j=1}^{n(i)} (f_{ij}^{cal} - f_{ij}^{exp})^2}{n(i)} \right) \tag{6}$$

Fig. 2 compares the thermograms and the differential thermograms recorded for experiments #10/4, #5 and #20 with those calculated with the best-fit values of the model parameters. The model describes the general trends of the thermograms qualitatively but shows large discrepancies with the experimental results, especially when two intermediate isothermal stages are included in the thermogram (experiment #20). We may therefore conclude that a better description of the interactions between lignin and phosphoric acid has to be incorporated into the model.

Analysis of the TG and DTG plots in Fig. 1 reveals some characteristic trends of the pyrolysis of lignin in the presence of phosphoric acid. Since water will evaporate at the lower temperature, the broad peak observed in the DTG between 100 and 450 °C in experiments #10/3, #4, #5 is not only caused by water evaporation but also by the decomposition of lignin and phosphoric acid. Water comes from the phosphoric acid solution, the moisture in lignin and from reactions of lignin and phosphoric acid at low temperature. In the presence of PA, lignin reacts through cleavage of the aryl–ether bonds, the formation of ketone groups, condensation and dehydration [20]. Pyrolysis of lignin in the presence of phosphoric acid shows that CO and CO_2 begin to evolve as volatile products at a temperature as low as 100 °C [21]. The inclusion of an isothermal stage at 150 °C for 60 min (experiments #5 and #20) shows that only 20% of the initial mass volatilizes at this temperature. This is attributed to the release of water and light compounds from lignin degradation by the action of phosphoric acid. When a second isothermal stage is included at 350 °C for 60 min (experiment #20), the total mass loss reaches 34%. The peak at 240–320 °C in the DTG curve for experiments #5 and #13 is attributed to the release of organic volatiles formed during the carbonization of the activated lignin. This peak is overlapped with the peak of water when no intermediate isothermal stage is used (experiments #10/3, #4, #5). When the sample is heated at 650 °C for 2 h, the final mass loss is around 62% for all experiments. The

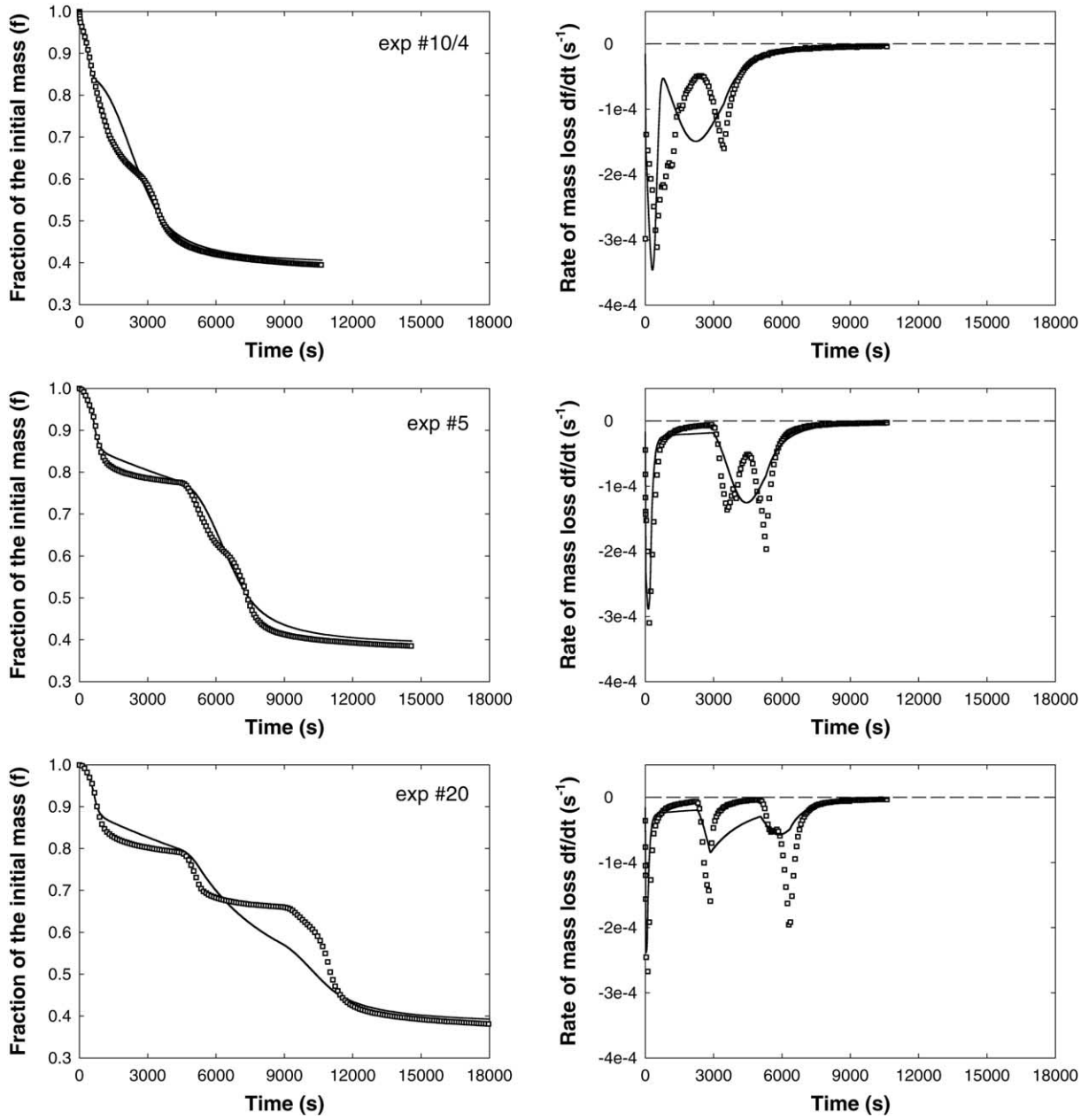

Fig. 2. Comparison between the experimental TG and DTG curves (□) and those calculated with the two parallel reactions kinetic model (–), Eqs. (1)–(5), for experiments #5, #10/4 and #20. (Experimental conditions listed in Table 2. For better visualization, only 1 data point out of 20 is plotted in the experimental TG and DTG curves.)

high degree of mass loss between 350 and 650 °C cannot be attributed to volatile matter from lignin alone since the rate of lignin pyrolysis reaches a maximum in the temperature interval from 300 to 370 °C [14,15]. The behavior of phosphoric acid at elevated temperature also has to be accounted for. The experiments presented in Fig. 1 were performed at a phosphoric acid-to-lignin mass ratio of 1.4:1, which exceeds the minimum ratio of 1.0:1.0 required to activate lignin completely [8]. As the temperature of the sample increases, the excess phosphoric acid is converted to pyrophosphoric acid ($H_4P_2O_7$) by condensation and dehydration. Extended heating forms polyphosphoric acid ($H_{n+2}P_nO_{3n+1}$), which finally decomposes to form P_2O_5, which sublimates above 300 °C and melts and vaporizes at 580–585 °C [22]. This temperature is very close to the peak observed at 650 °C in the DTG curves, which is therefore attributed to the volatilization of the P_2O_5.

4.1. Development of a new kinetic model for the pyrolysis of lignin activated with phosphoric acid

Qualitative interpretation of the thermograms leads us to the development of a kinetic model that accounts for the observed phenomena during the pyrolysis of lignin in the pres-

ence of phosphoric acid. The process was modeled with the reaction scheme described by Eqs. (7)–(12). Eq. (7) is the formation of a complex (LP) between lignin (L) and phosphoric acid (PA) through linkage of the phosphoric group to a reactive site in lignin. Based on experimental evidence we determined that this process finishes in 1 h at room temperature [8]. Therefore, this reaction was complete before the thermal treatment was started. Eq. (8) is the drying of the sample through water (WS) evaporation. Eq. (9) accounts for the conversion of the excess phosphoric acid to P_2O_5 (POS) when water is completely removed, and Eq. (10) describes the evaporation of POS. Finally, pyrolysis of the lignin–PA complex yields activated carbon (AC) and volatiles (VO), as described by Eq. (11). The parameter α indicates the mass fraction converted to activated carbon, and $(1-\alpha)$ indicates the mass fraction converted to volatiles during carbonization. Eq. (12) describes the partial volatilization of the activated carbon through slow pyrolysis to yield light gases (GA). All reaction rates were assumed to be first-order for each reactant.

$$\mathrm{L} + \mathrm{PA} \rightarrow \mathrm{LP} + \mathrm{WS}, \quad r_1 = \text{fast at room temperature} \tag{7}$$

$$\mathrm{WS} \rightarrow \mathrm{W}, \quad r_2 = k_2 C_{\mathrm{WS}} \tag{8}$$

$$\mathrm{PA} \rightarrow \tfrac{1}{2}(\mathrm{POS} + 3\mathrm{WS}), \quad r_3 = k_3 C_{\mathrm{PA}} \tag{9}$$

$$\mathrm{POS} \rightarrow \mathrm{PO}, \quad r_4 = k_4 C_{\mathrm{POS}} \tag{10}$$

$$\mathrm{LP} \rightarrow \alpha\mathrm{AC} + (1-\alpha)\mathrm{VO}, \quad r_5 = k_5 C_{\mathrm{LP}} \tag{11}$$

$$\mathrm{AC} \rightarrow \mathrm{GA}, \quad r_6 = k_6 C_{\mathrm{AC}} \tag{12}$$

Assuming that the reacting solid has homogeneous properties, individual mass balances are developed for each component of the solid:

$$\frac{\mathrm{d}f_{\mathrm{WS}}}{\mathrm{d}t} = -k_2 f_{\mathrm{WS}} + \frac{3}{2} k_3 \frac{\mathrm{MW_{WS}}}{\mathrm{MW_{PA}}} f_{\mathrm{PA}} \tag{13}$$

$$\frac{\mathrm{d}f_{\mathrm{PA}}}{\mathrm{d}t} = -k_3 f_{\mathrm{PA}} \tag{14}$$

$$\frac{\mathrm{d}f_{\mathrm{PO}}}{\mathrm{d}t} = -k_4 f_{\mathrm{PO}} + \frac{1}{2} k_3 \frac{\mathrm{MW_{PO}}}{\mathrm{MW_{PA}}} f_{\mathrm{PA}} \tag{15}$$

$$\frac{\mathrm{d}f_{\mathrm{LP}}}{\mathrm{d}t} = -k_5 f_{\mathrm{LP}} \tag{16}$$

$$\frac{\mathrm{d}f_{\mathrm{AC}}}{\mathrm{d}t} = \alpha' k_5 f_{\mathrm{LP}} - k_6 f_{\mathrm{AC}} \tag{17}$$

$$\alpha' = \alpha \frac{\mathrm{MW_{AC}}}{\mathrm{MW_{LP}}} \tag{18}$$

where f_j denotes the mass fraction of species j referred to the initial mass of the sample (M_0), MW_j is the molar mass of species j, and the rate of decrease of the fraction of the initial mass that remains in the solid ($\mathrm{d}f/\mathrm{d}t$) is obtained from Eq. (20). All the rate constants were assumed to follow the Arrhenius relationship Eq. (21).

$$f_j = \frac{M_j}{M_0} \tag{19}$$

$$\frac{\mathrm{d}f}{\mathrm{d}t} = \frac{1}{M_0} \sum_{j=1}^{5} \frac{\mathrm{d}M_j}{\mathrm{d}t} \tag{20}$$

$$k_i = k_{0_i} \exp\left(-\frac{E_i}{\mathrm{RT}}\right) \tag{21}$$

The initial mass-fraction composition of the sample was calculated from the amounts of phosphoric acid and lignin, the moisture content of the latter, and accounting for the water originated through reaction (1) (Eqs. (22)–(24))

$$f_{\mathrm{PA},0} = \frac{\left(\text{mass of anhydrous } \mathrm{H_3PO_4} - \text{mass of dry lignin}\left(\frac{\mathrm{MW_{PA}}}{\mathrm{MW_L}}\right)\right)}{\text{total mass}} \tag{22}$$

$$f_{\mathrm{LP},0} = \frac{\left(\text{mass of dry lignin}\left(\frac{\mathrm{MW_L} + \mathrm{MW_{PA}} - \mathrm{MW_W}}{\mathrm{MW_L}}\right)\right)}{\text{total mass}} \tag{23}$$

$$f_{\mathrm{WS},0} = \frac{\left(\text{mass of water} + \text{mass of dry lignin}\left(\frac{\mathrm{MW_{PA}}}{\mathrm{MW_L}}\right)\right)}{\text{total mass}} \tag{24}$$

The optimal values for the 12 unknown parameters in the model (k_{0_j}, E_j, α' and $\mathrm{MW_L}$) were estimated from the minimization of the least squares objective function F, Eq. (25), where n is the number of thermograms and $p(i)$ is the number of data points recorded for the ith thermogram (time, temperature fraction of the initial mass remaining and rate of mass loss). This objective function was chosen to simultaneously minimize the squared differences in the fraction of the initial mass remaining in the solid and the rate of mass loss. This was needed because it was observed that an objective function that was only based on the fraction of the initial mass gave optimal values that adjusted the data for the isothermal stages correctly, but gave poor results for the non-isothermal stages where the rates of mass loss were higher. Similarly, an objective function based on the rate of mass loss misrepresented the isothermal stages where the rate of mass loss was small.

The fraction of the initial mass remaining predicted by the model, $f(i,k)_{\mathrm{model}}$, was calculated with Eqs. (13)–(21), which were integrated numerically by an explicit Euler method. The temperature recorded at each sampling time along the thermogram was used to calculate the instantaneous rate constants. The rates of mass loss were evaluated numerically from the values of $f(i,k)$. This method provided a sufficient degree of accuracy because, as the thermograms were recorded at a high sampling frequency (typically one data point every 4 s), the time increments used in the calculations were small

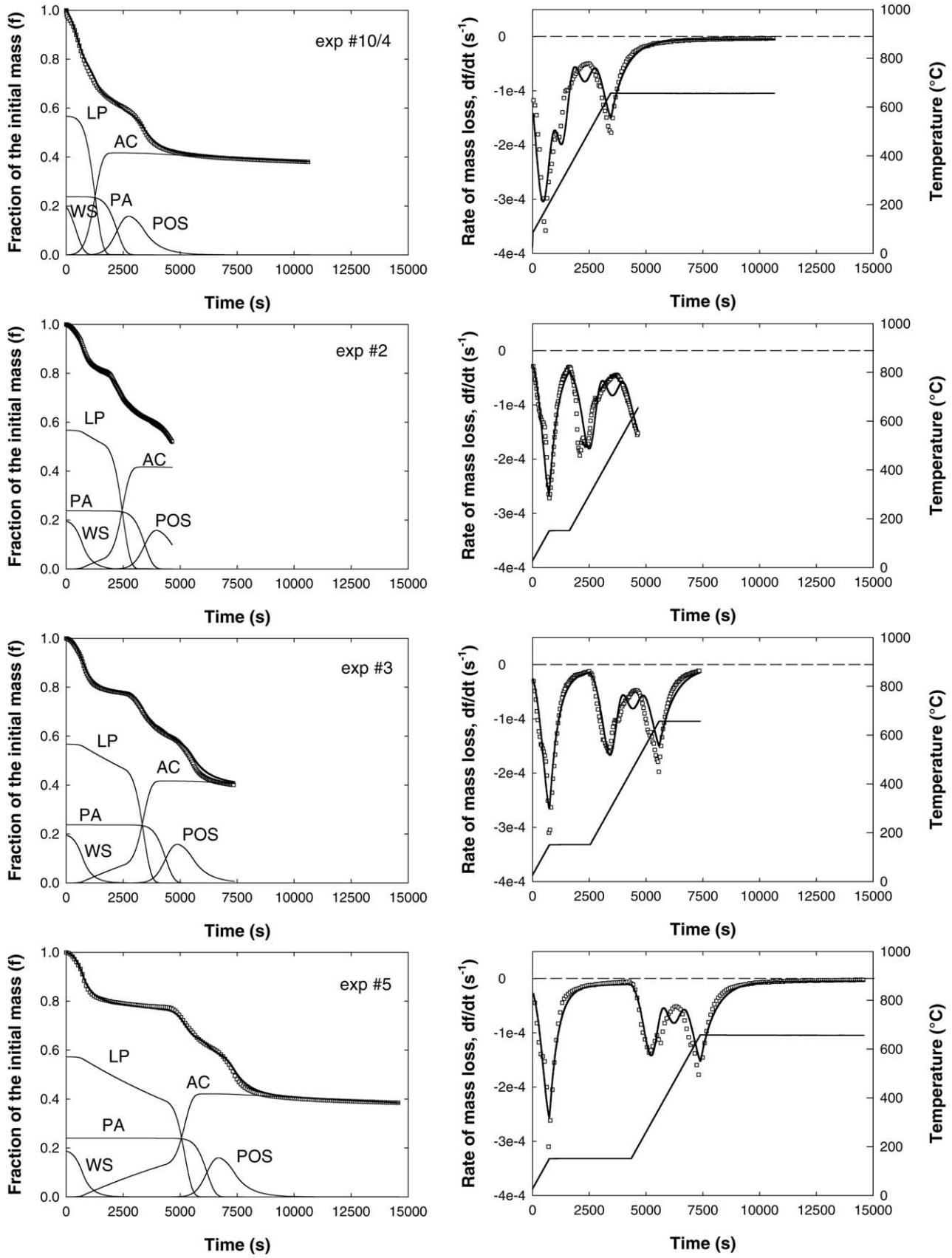

Fig. 3. Comparison between the experimental TG and DTG curves (□) and those calculated with the complete kinetic model (–), Eqs. (13)–(24), for experiments #2, #3, #5 and #10/4. (Experimental conditions listed in Table 2. Continuous thin lines are mass fractions calculated for lignin–phosphoric acid complex (LP), phosphoric acid (PA), water (WS), activated carbon (AC) and P_2O_5 (POS). For better visualization, only 1 data point out of 20 is plotted in the experimental TG and DTG curves.)

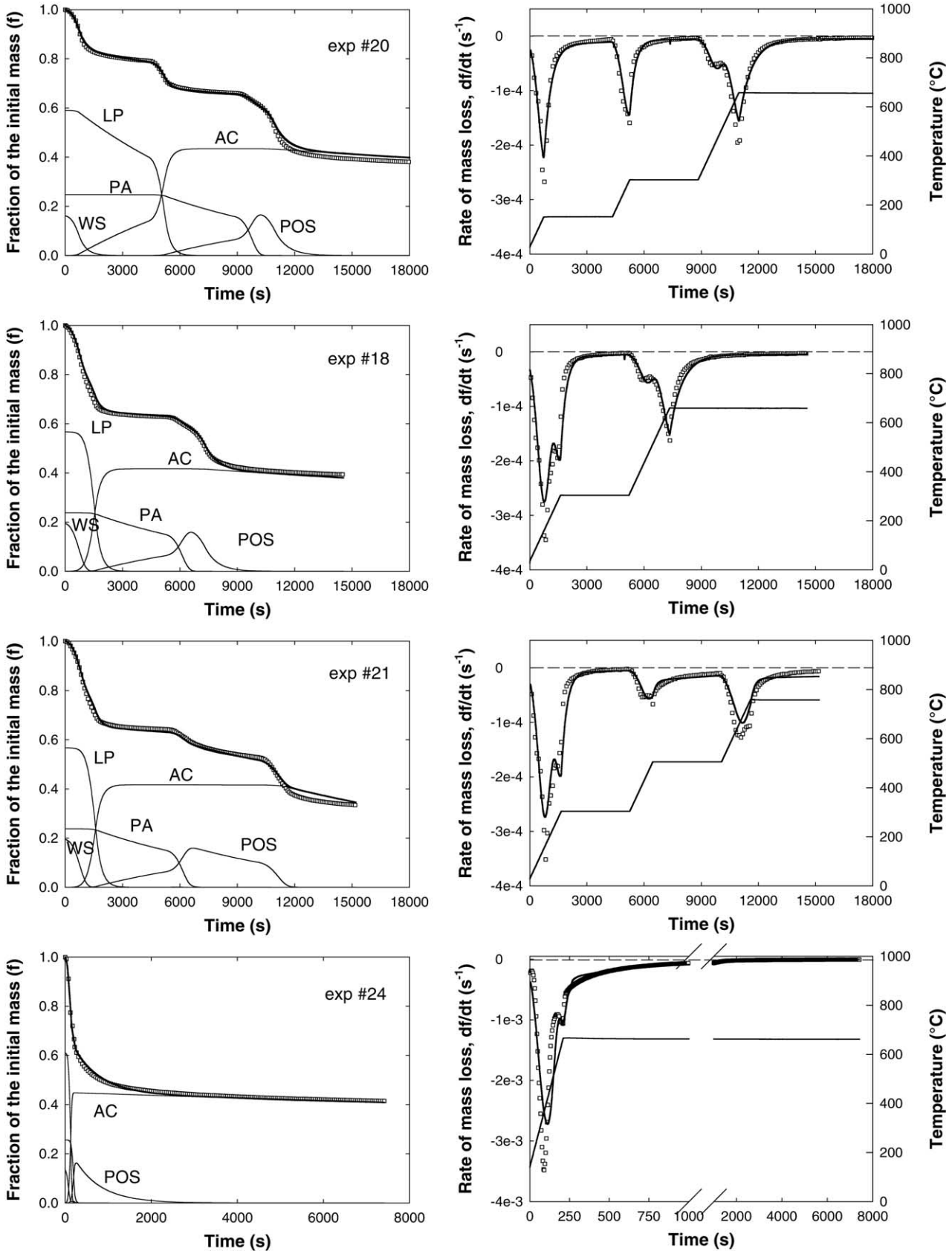

Fig. 4. Comparison between the experimental TG and DTG curves (□) and those calculated with the two parallel reactions kinetic model (–), Eqs. (13)–(24), for experiments #18, #20, #21 and #24. (Experimental conditions listed in Table 2. Continuous thin lines are mass fractions calculated for lignin–phosphoric acid complex (LP), phosphoric acid (PA), water (WS), activated carbon (AC) and P_2O_5 (POS). For better visualization, only 1 data point out of 20 is plotted in the experimental TG and DTG curves.)

Table 3
Least-squares best-fit values for the model parameters

Reaction	k_{0_j} (s^{-1})	E_j (kJ/mol)	MW_L (g/mol)	α'	Minimum F
(2)	4.20	26.0	135.3	0.736	2.205×10^{-2}
(3)	395.9	72.0			
(4)	326.4	95.0			
(5)	73.9	47.7			
(6)	11.1	106.3			

enough to avoid numerical instability.

$$F = \left(\sum_{i=1}^{n} \left(\frac{\sum_{k=1}^{p(i)} \left(\frac{f(i,k)_{\text{experimental}} - f(i,k)_{\text{model}}}{f(i,k)_{\text{model}}} \right)^2}{p(i)} \right) \right. \left. \sum_{i=1}^{n} \left(\frac{\sum_{k=1}^{p(i)} \left(\frac{\left(\frac{df(i,k)}{dt}\right)_{\text{experimental}} - \left(\frac{df(i,k)}{dt}\right)_{\text{model}}}{\left(\frac{df(i,k)}{dt}\right)_{\text{model}}} \right)^2}{p(i)} \right) \right)^{0.5} \quad (25)$$

The optimal values calculated for the activation energies (E_j), the frequency factors (k_{0_j}), the stoichiometric coefficient in reaction (5) (α') and the apparent molar mass of lignin (MW_L) are shown in Table 3. Activation energies were 26.0 kJ/mol for water desorption, 72.0 kJ/mol for the dehydration of phosphoric acid to phosphoric pentoxide, 95.0 kJ/mol for the volatilization of P_2O_5, 47.7 kJ/mol for the carbonization of the activated lignin and 106.3 kJ/mol for the pyrolytic release of light gases from activated carbon. The activation energy for the volatilization of lignin impregnated with phosphoric acid lies in the 35–100 kJ/mol range reported for lignin pyrolysis using several kinetic models [23], and falls below the range of activation energies from 60.6 kJ/mol at 200 °C to 153.6 kJ/mol at 700 °C reported for the pyrolysis of lignin activated with $ZnCl_2$ using a kinetic model based on a continuous distribution of activation energies [24]. Fig. 5 shows a sensitivity analysis for the influence of the model parameters on the least squares objective function F. This analysis shows that the activation energies (E_i), the apparent molar mass of lignin (MW_L) and the stoichiometric coefficient for the carbonization of the activated lignin (α') are evaluated accurately because the error function F is very sensitive to small variations in their individual values. The frequency factors (k_{0_i}) that we have calculated are more uncertain due to the low sensitivity of the error function to their value, especially for the frequency factor for the rate constants of phosphoric acid dehydration (k_3) and water volatilization (k_2).

Figs. 3 and 4 compare the thermograms measured for the experiments at an 85% phosphoric acid-to-lignin mass ratio of 1.4:1 (Table 2), and those calculated with the model using the best-fit values of the parameters. Agreement between the model and the experiments is excellent for all the thermograms, regardless of the number of intermediate isothermal stages. The same graphs also show the evolution of the mass fractions of water in the sample (WS), lignin–phosphoric acid complex (LP), phosphoric acid (PA), P_2O_5 (POS) and activated carbon (AC). Analysis of the temporal evolution of the mass fractions computed for each component in the solid mixture shows that drying of the sample (reaction (2)) takes place at the lowest temperature and is completed before the sample reaches 200 °C. Carbonization of the activated lignin (LP) starts at around 100 °C and is completed when the sample reaches 400 °C for the experiments without

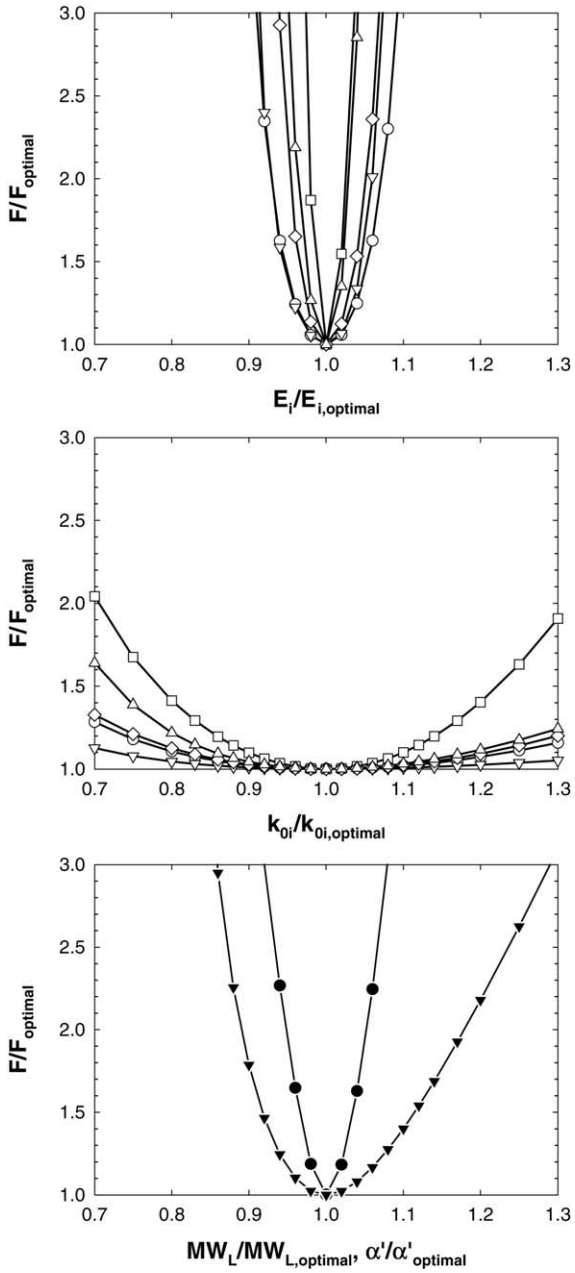

Fig. 5. Sensitivity analysis for the model parameters: activation energies (top), frequency factors (middle), and molar mass of lignin, MW_L, and α' (bottom) (E_1, k_1: ○; E_2, k_2: ▽; E_3, k_3: □; E_4, k_4: ◇; E_5, k_5: △; α': ▼; and MW_L: ●).

intermediate isothermal stages (experiment #10/4), or with an isothermal stage at 150 °C for 60 min (experiment #5), but reaches completion at 300 °C if an isothermal stage at 300 °C for 60 min is included in the temperature program (experiment #18). Decomposition and volatilization of the excess phosphoric acid take place at a higher temperature and are responsible for the mass loss observed above 400 °C. This starts at around 230 °C, which is close to the value of 213 °C reported for pure orthophosphoric acid [22], and is completed at around 550–580 °C. This broad interval of reaction temperature agrees qualitatively with the consecutive reactions involved in the formation of P_2O_5 from phosphoric acid, which proceeds through the formation of pyrophosphoric acid ($H_4P_2O_7$), polyphosphoric acid ($H_{n+2}P_nO_{3n+1}$) and finally P_2O_5. The volatilization of phosphorous pentoxide also happens in a broad interval of temperature. According to the kinetic model, it starts once the sample reaches around 280 °C, which is close to its sublimation temperature of 300 °C, and takes place much faster above 570 °C when vaporization is accelerated due to the melting of P_2O_5 at 580–585 °C [22]. Finally, the residual mass loss during the isothermal stage at 650 °C is caused by the release of light

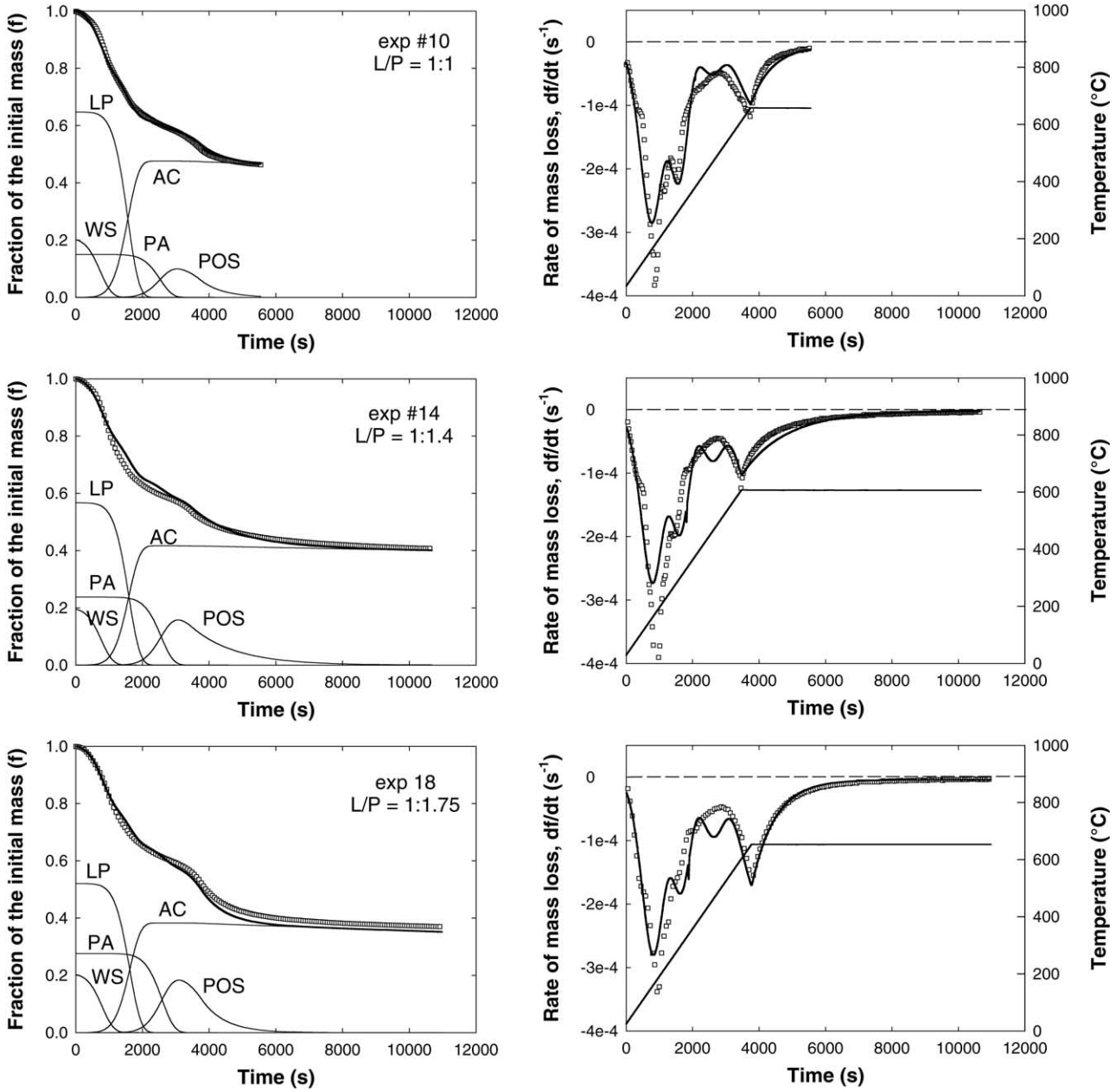

Fig. 6. Comparison between the experimental TG and DTG curves (□) and those calculated with the two parallel reactions kinetic model (–), Eqs. (13)–(24), for experiments #10 L/P 1:1.0, #14 L/P 1:1.4 and #18 L/P 1:1.75. (Experimental conditions listed in Table 2. Continuous thin lines are mass fractions calculated for lignin–phosphoric acid complex (LP), phosphoric acid (PA), water (WS), activated carbon (AC) and P_2O_5 (POS). For better visualization, only 1 data point out of 20 is plotted in the experimental TG and DTG curves.)

gases as the carbon formed at lower temperatures is pyrolyzed to a greater extent.

Analysis of the differential thermograms, also presented in Figs. 3 and 4, shows that the model accurately describes the rate of mass loss for the experiments with one intermediate isothermal stage at 300 °C (#18, #20, #21). Four maximums in the rate of weight loss are observed: the first for water volatilization, the second for the release of volatiles during the formation of activated carbon, the third for the decomposition of phosphoric acid and the fourth for the volatilization of P_2O_5. For the other experiments there are some discrepancies in the temperature interval from 300 to 500 °C since the model shows the existence of a small maximum on the rate of mass loss at around 450 °C caused by phosphoric acid dehydration to phosphorous pentoxide, which is not observed experimentally. Close examination of the experimental rate of mass loss in this temperature range shows a series of small maximums and inflection points (see experiments #2 and #3, for instance), which point to the existence of a set of simultaneous reactions taking place in the solid. These reactions are probably related to the decomposition of phosphoric acid to P_2O_5, which in the model has been assumed to proceed through a single reaction step (Eq. (9)), though, as described before, it actually proceeds through a series of consecutive steps (Fig. 5).

The influence of the PA-to-lignin ratio is examined in Fig. 6, which shows the results for experiments performed at PA-to-lignin ratios of 1.0:1.0, 1.4:1.0 and 1.75:1.0 (w:w) using similar temperature profiles throughout the experiment. The model can reproduce the measured thermograms within the limits of the experimental error in all cases, thus proving its robustness. Analysis of the differential thermograms show limitations for the three experiments similar to those noted earlier: the model can describe the general trends in the temporal evolution of the rate of mass loss but there are minor discrepancies in the temperature interval from 300 to 500 °C caused by the complex nature of the reactions involved in phosphoric acid decomposition.

5. Conclusions

A phenomenological kinetic model has been developed for the pyrolysis of lignin activated with phosphoric acid at low heating rates to produce activated carbon. The model is based on TG and DTG data from pyrolysis experiments and it assumes that lignin carbonization proceeds through a set of pseudo-first-order reactions. These reactions are a simplified description of the multiple reaction processes involved in the thermal decomposition of lignin mixed with an excess of phosphoric acid. The model provides a good representation of the thermograms regardless of the phosphoric-acid-to-lignin ratio and the temperature profile along the reaction. The activation energies and other parameters have been calculated from the experimental mass-loss and differential mass-loss curves. The model could be improved if the composition of the volatile products were analyzed continuously by on-line mass spectrometry to determine the actual rates of volatilization for water, phosphoric acid-derived products (i.e., P_2O_5) and carbon-containing compounds.

Acknowledgements

The authors are indebted to the Catalan Regional Government and the Spanish Government for financial support (projects 2001SGR-00323 and PPQ2002-04201-CO2-02, respectively). Vanessa Torné-Fernández is grateful to the Rovira i Virgili University (URV) for a PhD scholarship.

References

[1] T. Vernersson, P.R. Bonelli, E.G. Cerrella, A.L. Cukierman, *Arundo danax* cane as precursor for activated carbons preparation by phosphoric acid activation, Biores. Technol. 83 (2002) 95–104.
[2] V.D. del Bagno, R.L. Miller, J.J. Watkins, On site production of activated carbon from Kraft Black Liquor, US EPA Report 600/2-78-191, 1978.
[3] J. Rodríguez-Mirasol, T. Cordero, J.J. Rodríguez, Preparation and characterization of activated carbons from eucalyptus kraft lignin, Carbon 31 (1993) 87–95.
[4] E. González Serrano, T. Cordero, J. Rodríguez-Mirasol, J.J. Rodríguez, Development of porosity upon chemical activation of Kraft lignin with $ZnCl_2$, Ind. Eng. Chem. Res. 36 (1997) 4832–4838.
[5] H. Teng, T.S. Yeh, L.Y. Hsu, Preparation of activated carbon from bituminous coal with phosphoric acid activation, Carbon 36 (1998) 1387–1395.
[6] J. Hayashi, A. Kazehaya, K. Muroyama, P. Watkinson, Preparation of activated carbon from lignin by chemical activation, Carbon 38 (2000) 1873–1878.
[7] V. Fierro, V. Torné-Fernández, D. Montané, R. Garcia-Valls, Removal of Cu (II) from aqueous solutions by adsorption on activated carbons prepared from Kraft lignin, in: A. Linares-Solano, D. Cazorla-Amorós (Eds.), Proceedings of Carbon 2003, Oviedo, Spain.
[8] V. Fierro, V. Torné-Fernández, D. Montané, J. Salvadó, Activated carbons prepared from Kraft lignin by phosphoric acid impregnation, in: A. Linares-Solano, D. Cazorla-Amorós (Eds.), Proceedings of Carbon 2003, Oviedo, Spain.
[9] S.H. Yoon, B.C. Kim, Y. Korai, I. Mochida, Multi-staged carbonization of aramid fibers, in: Proceedings of the 22nd Biennial Conference on Carbon, Extended Abstract and Program, San Diego, CA, 1995, p. 218.
[10] C. Pastor, F. Rodríguez-Reinoso, H. Marsh, M.A. Martínez, Preparation of activated carbon cloths from viscous rayon. Part I. Carbonization procedures, Carbon 37 (1999) 1275–1283.
[11] F. Suárez-García, A. Martínez-Alonso, J.M.D. Tascón, Pyrolysis of apple pulp: effect of operation conditions and chemical additives, J. Anal. Appl. Pyrolysis 62 (2002) 93–109.
[12] G. Varhegyi, M.J. Antal, Kinetics of the thermal decomposition of cellulose, hemicellulose and sugar cane bagasse, Energy Fuels 3 (1989) 329–335.
[13] J.J. Manyà, E. Velo, L. Puigjaner, Kinetics of biomass pyrolysis: a reformulated three-parallel-reactions model, Ind. Eng. Chem. Res. 42 (2003) 434–441.
[14] J.A. Caballero, A. Marcilla, J.A. Conesa, Thermogravimetric analysis of olive stones with sulphuric acid treatment, J. Anal. Appl. Pyrolysis 44 (1997) 75–88.
[15] J.J.M. Órfão, F.J.A. Antunes, J.L. Figueiredo, Pyrolysis kinetics of lignocellulosic materials - three independent reactions model, Fuel 78 (1999) 349–358.

[16] J.J.M. Órfão, J.L. Figueiredo, A simplified method for determination of lignocellulosic materials pyrolysis kinetic from isothermal thermogravimetric experiments, Thermichim. Acta 380 (2001) 67–78.
[17] D. Vamvuka, E. Kakaras, E. Kastanaki, P. Grammelis, Pyrolysis characteristics and kinetics of biomass residuals mixtures with lignite, Fuel 82 (2003) 1949–1960.
[18] V. Cozzani, L. Petarca, L. Tognotti, Devolatilization and pyrolysis of refuse derived fuels: characterization and kinetic modeling by a thermogravimetric and calorimetric approach, Fuel 74 (1995) 903–912.
[19] C.A. Koufopanos, G. Maschio, A. Lucchesi, Kinetic modeling of the pyrolysis of biomass and biomass components, Can. J. Chem. Eng. 67 (1989) 75–84.
[20] Y.Z. Lai, in: D.N.S. Hon, N. Shirashi (Eds.), Chemical Degradation in Wood and Cellulose Chemistry, vol. 10, Marcel Dekker, New York, 1991, p. 455.
[21] M. Jagtoyen, F. Derbyshire, Activated carbons from yellow poplar and white oak by H_3PO_4 activation, Carbon 36 (1998) 1085–1097.
[22] D.R. Lide (Ed.), Handbook of Chemistry and Physics, 72nd ed., CRC Press, Boca Raton, FL, 1991.
[23] R.K. Sharma, J.B. Wooten, V.L. Baliga, X. Lin, W.G. Chan, M.R. Hajaligol, Characterization of chars from pyrolysis of lignin, Fuel (2004) (Corrected proof, available online 25 March).
[24] E. Gonzalez-Serrano, $ZnCl_2$—chemical activation of kraft lignin, PhD Dissertation, University of Málaga, Málaga, Spain, 1996.